Progress In Electromagnetics Research, PIER 56, 53–66, 2006

A NEW TECHNIQUE TO FIND THE MEI COEFFICIENTS IN THE TIME DOMAIN: "SELF-METRON TECHNIQUE"

R. Pazoki and A. Cheldavi

College of Electrical Engineering
Iran University of Science and Technology
Tehran, Iran

Abstract—Measured equation of invariance in the time domain (TD-MEI) has been used as an FDTD-ABC. The TD-MEI coefficients, are derived using a new technique named "self metron". Unlike the traditional MEI, in this technique there is no need to use metrons to find the MEI coefficients. The real field values of the same FDTD problem but with a PEC surface instead of a radiation boundary condition are sampled and used to find the MEI coefficients. The key is to locate the PEC mesh truncation, farther away than the MEI truncation boundary, such that during the sampling time interval, no wave reflects into the MEI truncation boundary. After the MEI coefficients are found, according to the "time invariance" property of the TD-MEI coefficients, the MEI boundary absorbs the wave for all times. The proposed technique is very fast and the results show that the accuracy is much higher than traditional absorbing boundary conditions and some other ABC's.

1. INTRODUCTION

Since the advent of the measured equation of invariance, the most of the effort is devoted to frequency domain problems. Thereafter it was approved that the MEI coefficients can be also used in the time domain [1]. In further works, it was shown that the MEI coefficients, which are postulated to be "invariant with time", can be numerically determined by using the analytical solutions of the wave equation [2]. The derived analytical solutions are not the actual values of the fields in the related problem. These values are derived from choosing some arbitrary current distributions (metrons) on the scatterer based on the third postulate of MEI [3]. In the proposed technique in the present paper, the MEI coefficients are calculated from the actual field values

which are generated by the actual excitation, using the FDTD solution of the same problem up to necessary time and space steps. The values of the real fields of the same problem are found using FDTD with a PEC surface instead of a radiation boundary condition. These values are then sampled and used to find the MEI coefficients. The most important key is to locate the PEC mesh truncation, farther away than the proposed MEI truncation boundary. This ensures that during the sampling time interval, no wave reflects into the MEI truncation boundary. After the MEI coefficients are found, according to the "time invariance" property of the TD-MEI coefficients, the MEI boundary absorbs the wave for all times.

The advantages of this method over the traditional MEI are:

1- The accuracy of this method is much more than traditional MEI.

2- The MEI coefficients can be derived easier and faster than traditional MEI.

3- Since the MEI coefficients are derived from the actual excitation, it terminates the debates concerning MEI's third postulate [4].

4- This method is suitable and can be applied not only for PEC's objects but also for the objects of inhomogeneous and anisotropic materials with arbitrary geometry, without resorting to the complicated Green's function of the related constructions.

Two examples support the accuracy of the proposed technique: The first one shows the TM radiation of an infinite line source, and the self metron results are compared with that of the traditional MEI, PML and Mur2 ABC's. The second example shows the scattering from a circulant microstrip line, and the self metron results are compared with that of a 10-layer UPML.

2. SUMMARY OF THE TRADITIONAL MEI APPROACH

The MEI equations in the time domain is expressed as follows [5]:

$$\sum_{j\in S}\sum_{m\in T(j)} a_{j,m}\phi_j^m = 0 \tag{1}$$

Where $T(j)$ is a series of time steps, S is a set of field points near the truncated boundary node i, and ϕ_j^m is a set of field values. $a_{j,m}$, is a set of MEI coefficients to be determined by a series of known ϕ_j^m named measuring functions, which should satisfy Maxwell's equations.

In fact many truncated boundary conditions can be summarized by equation (1). Experiments show that the nodes distributed along

a straight line which is perpendicular to the boundary, as shown in Figure 1, provide absolute stability for equation (1). The form of equation (1) applied in this paper is:

$$\phi_i^{n+1} = a_1\phi_{i-1}^{n+1} + a_2\phi_i^n + a_3\phi_{i-1}^n \tag{2}$$

Which is referred to as the first MEI relationship. In two-dimensional coordinate systems, the radiation field of a line source $J(\vec{r}_0, t)$ positioned at $\vec{r}_0$ is

$$\phi(\vec{r}, t) = \int_{-\infty}^{+\infty} G(\vec{r}, \vec{r}_0; t, t')\frac{\partial}{\partial t'}J(\vec{r}_0, t')dt' \tag{3}$$

Where $G(\vec{r}, \vec{r}_0; t, t')$ is the Green's function in the time domain

$$G(\vec{r}, \vec{r}_0; t, t') = \frac{C}{2\pi\sqrt{C^2(t-t')^2 - |\vec{r} - \vec{r}_0|^2}}H[C(t-t') - |\vec{r} - \vec{r}_0|] \tag{4}$$

And H is the Heaviside function, and C is the wave velocity in free space. In TDMEI, $J(\vec{r}_0, t)$ need not be the true current distribution, and can be chosen arbitrarily to obtain the measuring functions. After the choice of measuring currents, a series of ϕ_j^m is obtained and substituted into equation (2). In order to find 3 MEI coefficients in equation (2), one needs 3 set of known solutions of ϕ at least. These solutions can be obtained from 3 different time steps (measuring interval) that satisfy equation (2). To get to better and more accurate coefficients one needs to take more equations and utilizing the least squares method to find the MEI coefficients.

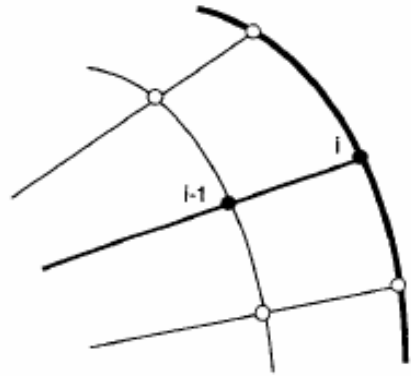

Figure 1. Nodes in TDMEI equation.

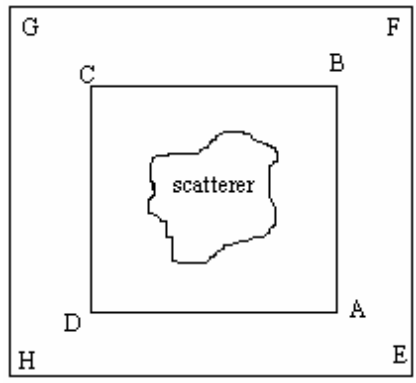

Figure 2. Configuration of the problem to find the MEI coefficients using the self-metron technique.

3. THE SELF METRON METHOD PRINCIPLES

For the TM case, the first MEI relation has the following form [6]:

$$E_z^{n+1}(i) = a_1 E_z^{n+1}(i-1) + a_2 E_z^n(i) + a_3 E_z^n(i-1) \tag{5}$$

As it was demonstrated, the required sampling time interval to obtain the first MEI coefficients should be more than 3 time steps. According to the time invariance of the MEI coefficients, the end of the sampling time can be before the end of the simulation time. Once the MEI coefficients are found, the MEI-ABC absorbs the wave for all times.

Assume that we want to simulate the configuration shown in Figure 2, using the FDTD method with the MEI-ABC. Our intent is to find the MEI coefficients and use the MEI-ABC on the ABCD boundary near the object. First we set the exterior walls as PEC and locate them on the EFGH boundary, and run the FDTD code with this configuration. When the wave reaches to the ABCD boundary, we sample the field values (measures) on the ABCD nodes and their interior immediate neighbors. The sampling time should be more than 3 time steps, and during this interval, no wave should reflect from the PEC surface (EFGH surface) into the MEI boundary. Then, when the known solution sets are obtained, the MEI coefficients can be derived by use of the least squares method.

4. EXAMPLE 1: RADIATION OF A LINE SOURCE

4.1. Simulation Data

The configuration of the problem is shown in Figure 3. An infinite line source with a Gaussian distribution is positioned at the point S. The distribution of the pulse is chosen like that of used in [6], and is as follows:

$$f(t) = \begin{cases} \dfrac{\exp[-10(2F_b t - 1)^2] - e^{-10}}{1 - e^{-10}} & 0 \le t \le \dfrac{1}{F_b} \\ 0 & t > \dfrac{1}{F_b} \end{cases} \tag{6}$$

We choose the problem conditions exactly like [6]. The size of the square meshes are chosen as $\Delta x = \Delta y = \lambda_{\min}/20$, in which $\lambda_{\min} = C/F_b$ (F_b is the highest frequency component of the pulse $\Delta t = \Delta x/(2C) = 1/(40F_b)$, and $N_x = N_y = 10$. The test point M is positioned in the middle of the line BP. We choose the region EFGH (with PEC walls) large enough so that until the end of the simulation time, no reflected wave enters into the ABCD region. In order to find the MEI coefficients, the measuring interval is chosen 20 time steps, (the time width of the pulse is 40 time steps), considering the distance between ABCD walls (Fig. 3) and the line source which is 9 nodes, the final sampling time will be $18 + 20 = 38$ time steps. In order to prevent the reflected wave from PEC walls (EFGH in Fig. 3), the distance between ABCD and EFGH should be at least 5 nodes. In this case, since there is no reflection error due to absorbing boundary conditions, we call it "no reflection" case. The self-metron results are compared with that of given in [6].

4.2. Error Analysis and Numerical Results

The self-metron case is compared with the traditional MEI. The error at node M at different time steps, and the error on the boundary nodes at a specific time step, and the total reflection error in the whole region (global error) are measured.

4.3. Error on a Fixed Node at Different Time Steps

The distance between node M and the source is nearly 10 nodes. So it takes 20 time steps that the pulse reaches to the point M. Since the time width of the pulse is 40 time steps, it totally takes 60 time steps that the pulse leaves the simulation region. We therefore, compare the results with NR (no reflection) case before the time step 60, and

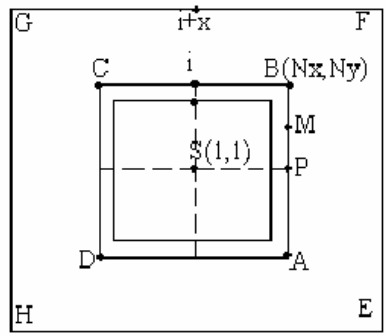

Figure 3. Configuration of radiation of a line source.

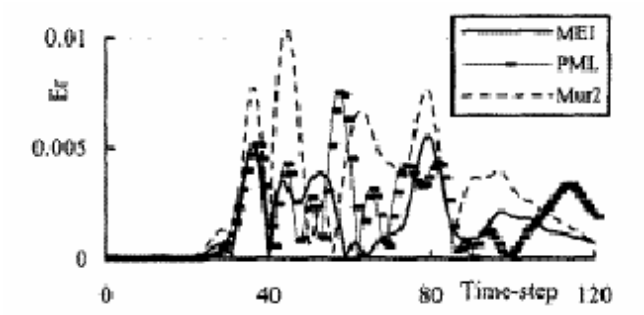

Figure 4a. *E*-field reflection error due to traditional MEI, PML and Mur2 at point M.

thereafter, the results are compared with zero (the exact value). We define the reflection error as follows:

$$Er(i,j) = |Er(i,j)_{NR} - Er(i,j)_{MEI}| \tag{7}$$

Figure 4a shows the results obtained from [6], and Figure 4b shows the result obtained from the self-metron MEI technique. Comparison shows that the accuracy of self-metron MEI is higher than the traditional MEI, PML-ABC (with 8 layers), and Mur2.

After the time step 60, when the pulse totally leaves the simulation region, the exact field values at point M should be zero. The computed filed values using NR and self metron methods are shown in Figure 5. Since after this time step, the pulse has totally left this point, the residual field values shown in Figure 5 are error. As it can be seen, the MEI results are even better than the no-reflection results. It is known that there is a numerical dispersion error in the FDTD analysis which

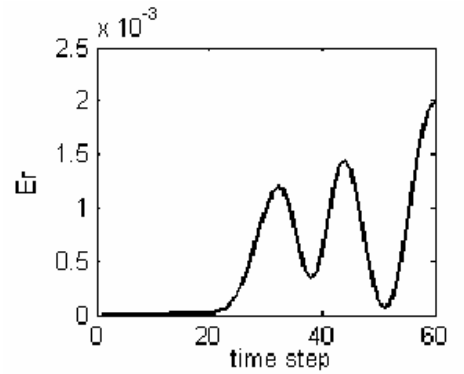

Figure 4b. E-field reflection error due to self-metron MEI method at point M.

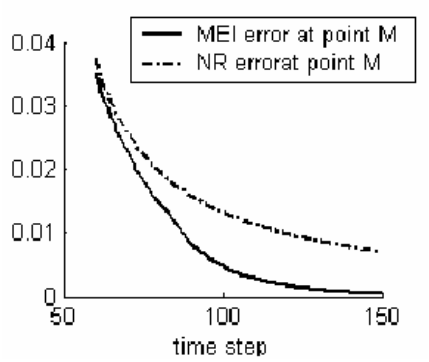

Figure 5. Numerical error, resulted from the self-metron MEI and no reflection cases, the time step 60, when the pulse totally leaves the simulation region.

is proportional to the size of the simulation region. However, MEI is a dispersion-free relation (frequency independent) and since the region simulated by the MEI method is smaller than that of no reflection, there is smaller error due to the dispersion in the MEI case.

4.4. Observation of All Nodes at a Fixed Moment

At $t = 38\Delta t$, the pulse has its maximum value in the truncation boundary. The reflection error at side APB resulted from the traditional and self-metron MEI are shown in Figures 6a and 6b respectively. It can be seen that the self-metron error is much less

than the results in [6].

4.5. Total Error in the Whole Simulation Region

The total reflection error (global error) is defined as follows [6]:

$$TEr = \sum_i \sum_j |Er(i,j)|^2 \tag{8}$$

Figures 7a and 7b show the results of [6] and the self-metron MEI respectively. It is obvious that the self-metron MEI is more accurate.

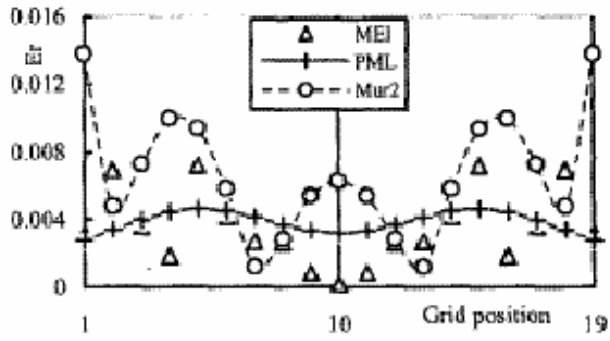

Figure 6a. Reflection error at side APB at $t = 38\Delta t$ resulted from different methods [6].

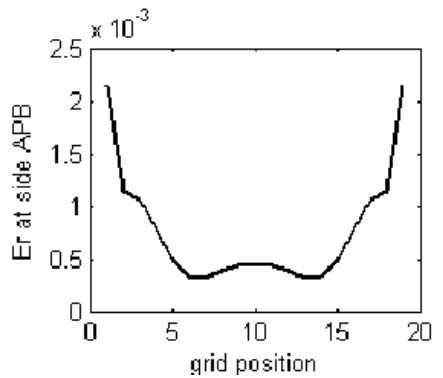

Figure 6b. Reflection error at side APB at $t = 38\Delta t$ resulted from the self-metron MEI.

5. EXAMPLE 2, SCATTERING PROBLEMS

5.1. Simulation Data

The source is a TM-polarized Gaussian plane wave pulse with $\Delta t = 1/120Fb$. The structure is a circulant symmetric microstrip line [7], as shown in Figure 8.

The outer and inner radius of the dielectric are $r_{out} = \lambda_{\min}/2$ and $r_{in} = \lambda_{\min}/4$ respectively. The mesh size is $\Delta x = \Delta y = \lambda_{\min}/10$, and the relative permittivity of the dielectric, ε_r is 4. Two absorbing boundary conditions, i.e. the MEI-ABC and the UPML are compared. The MEI-ABC is located 24 nodes away from the center of the simulation region, and for the UPML case, a 10 cell quadrically graded

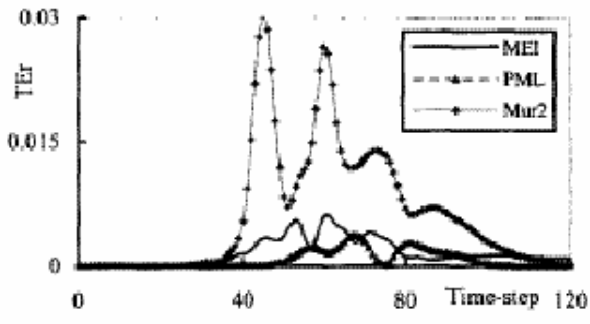

Figure 7a. Total reflection error resulted from traditional MEI and etc. in the ABCD region (19 by 19 nodes).

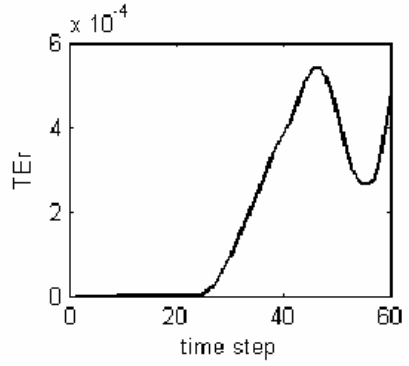

Figure 7b. Total reflection error resulted from self-metron MEI method in the ABCD region.

UPML [8], has filled the region between ABCD and EFGH boundaries. The MEI coefficients are derived using the self-metron technique. The end of the sampling time is 150 time steps.

With respect to the given data of the problem, it can be calculated that the extra layer to be added to prevent the reflacted wave from PEC walls, should be about 15 nodes. this extra layer just leads to a few more seconds comparing the problem size with ABCD borders, and is used to collect the measuring functions.

Here we again emphasize that the end of the sampling time is very sooner than the end of the simulation time, so it should not lead to the misconception that to find the MEI coefficients we have solved the problem first.

5.2. Error Analysis and Numerical Results

The error is compared with the no-reflection case. The error at fixed nodes at different moments and the total error in the whole simulation region is analyzed.

5.2.1. Error at Different Moments at Fixed Nodes

The error is defined like (7) and is analyzed at four different nodes (Figure 8), at the points $M1$ (the middle of the line AB), $M2$ (the middle of the line $M1B$), $M3$ (the middle of the line CD), and $M4$ (the middle of the line $M3D$). Figures 9a to 9d show the reflection error of the MEI and UPML ABC's until the time step 250. The accuracy of the MEI-ABC is higher in all cases. Although the end of the sampling

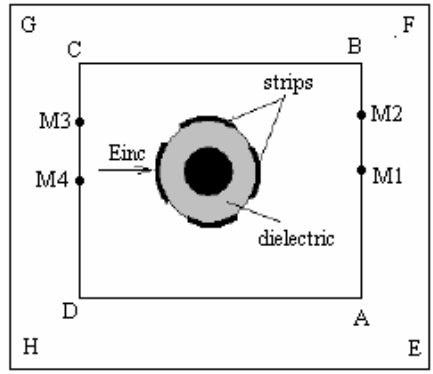

Figure 8. Scattering from circulant symmetric microstrip line structure.

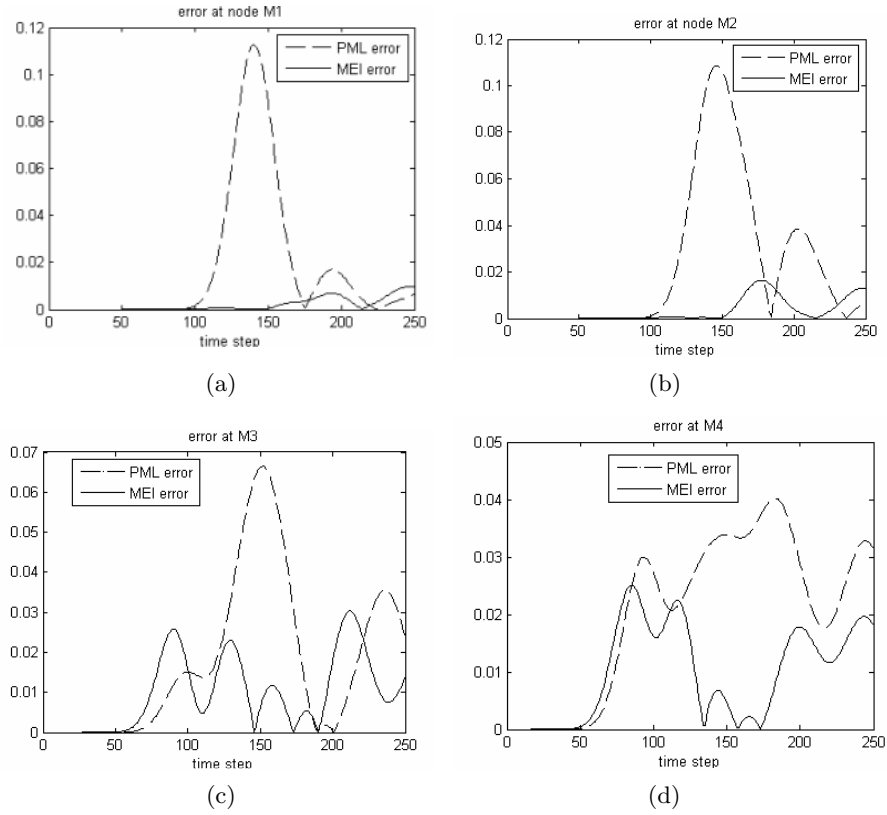

Figure 9. Error at fixed points at different moments, resulted from the MEI and UPML ABC's.

time is 150 time steps, it is obvious that the MEI-ABC almost absorbs the wave after the time step 150, and it confirms the time invariance of the measured equation of invariance. In practice, the scattered fields suffer reflections in the interior of dielectric objects. It is not practical to simulate these reflections in the no-reflection case, because to avoid the reflections from the PEC walls to the boundaries (i.e., MEI or PML) the simulation region should be very large. Therefore after the time step 250, The MEI-ABC is compared directly with UPML.

Figure 10 shows the absolute difference of the E_z field values at points M1 and M4 respectively. It is obvious that the results are close to each other.

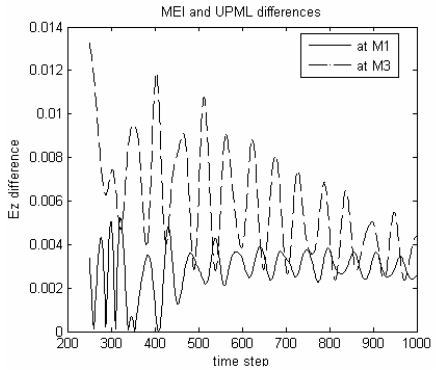

Figure 10. Absolute differences of the E_z field values using the MEI and UPML ABC's.

5.2.2. Total Error in the Whole Simulation Region

The total error (global error) is defined the same as (8). Fig. 11 shows the global error of the self metron MEI and UPML ABC's. It is evident that self metron global error is much less than the UPML. It is worth noting that since in the UPML case a 10 spurious layer is implemented, and the FDTD technique uses intermediate field values [8], the simulation time as well as memory requirements is much more than the MEI case (especially in 3-D case). However unlike the UPML, the MEI-ABC is structure dependent, so by changing the structure we have to recalculate the MEI coefficients.

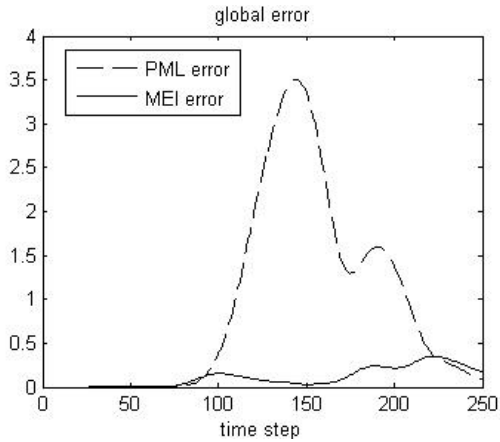

Figure 11. Self metron MEI and UPML global errors.

6. CONCLUSION

A novel technique to find MEI coefficients in the time domain was introduced. Since the original problem has been used, there is no need to more pre-processing calculations to find the measuring functions. Therefore the MEI coefficients can be calculated using this method very easier than the traditional MEI. It is known that the MEI coefficients are invariant to the excitation. But it is also well known that the MEI error is dependent to the mesh size (h) as $O(h^2)$. So, by changing the spectrum of the excitation, the actual mesh size (h) will be changed and hence, the error may increase. So it is better to find the MEI coefficients using the actual excitation. Unlike the traditional MEI, we do not need to find the complicated time domain Green's function of the structure under consideration. Because the simulation is terminated very close to the object surface, and the simulation region is smaller than the other methods, the numeric dispersion error, as well as the time and memory requirements in self metron MEI method, is much less than the other methods.

REFERENCES

1. Mei, K. K. and Y. W. Liu, "On time domain measured equation of invariance," *URSI Meeting Seattle, Washington State*, June 1994.
2. Liu, Y. W., K. K. Mei, and K. N. Yang, "Measured equation of invariance in time domain," *IEEE Asia Pacific Microwave Conference*, 1997.
3. Mei, K. K., R. Pous, Z. Chen, Y. Liu, and M. D. Prouty, "The measured equation of invariance — A new concept in field computation," *IEEE Trans. on Ant. and Prop.*, Vol. 42, No. 3, March 1994.
4. Jevtic, J. O., "How invariant is the measured equation of invariance?" *IEEE Microwave and Guided Wave Letters*, Vol. 5, No. 2, Feb. 1995.
5. Liu, Y., K. Lan, C. Liao, and K. K. Mei, "Time domain MEI method for radiation of a line source," *IEE, Electronic Letters*, Jan. 1999.
6. Liao, C., L. Meng, D. Yang, and X.-M. Zhong, "Analysis of the numerical error for time domain MEI absorbing boundary condition," *Proceedings of APMC*, Taipei, Taiwan, 2001.
7. Cheldavi, A. and M. Khalaj Amirhosseini, "Analysis of circulant symmetric coupled strip lines," *J. of Electromagnetic Waves and Appl.*, Vol. 16, No. 7, 977–994, 2003.

8. Taflove, A. and S. C. Hagness, *Computational Electrodynamics: The Finite Difference Time Domain Method*, 2nd edition Artech House, 2000.